Capacitor Discharge Welding: Analysis through Ultrahigh-Speed Photography

High-speed examination of the weld reveals metal expulsion caused by plasma jet of the cathode

BY R. D. WILSON, J. R. WOODYARD, SR., AND J. H. DEVLETIAN

ABSTRACT. Ultrahigh-speed photography of 44,000 frames/s was used to investigate the capacitor discharge welding (CDW) process. The objective of the study was to use high-speed photography and a finite element computer program to help describe the heat flow characteristics of the CDW cycle. The photos revealed that the plasma jet from the cathode was responsible for expelling metal from the anode rather than being squeezed out on contact. Photographic evidence suggested that the unequal anode/cathode heating ratio is primarily due to heat transfer from the anode to the expelled metal particles.

Introduction

Ultrahigh-speed photography was used to observe several transient phenomena taking place during the process of capacitor discharge welding (CDW). Contrary to accepted theory, these photographs reveal for the first time that material is dynamically expelled from the weld by a plasma jet phenomenon rather than being squeezed out upon contact. An explanation is presented to explain the difference in energy partitioning between the two electrodes observed during the CDW process and the apparent lack of correlation between dissipation energy, arc duration, and weld spatter.

Capacitor discharge (CD) welding has become a valuable technique for studying methods of joining parts made from rapidly solidified materials. Rapid solidification processing (RSP) alloys have shown great promise for creating advanced materials applicable to various engineering problems. These materials are quenched at rates so high (>10^3 K/s) that metastable phases, ultrafine grain structures, and particularly interesting solidification structures may be retained by the material at ambient temperatures. In order for RSP to be effective, at least one dimension of the material being processed must be extremely small (on the order of 10^4 m or less). As a result, RSP materials are made in the form of ribbons, fibers, or powders. To retain the desirable RSP properties, such materials must be consolidated using techniques that do not alter the material's previous thermal history. Usually, such materials are consolidated using hot extrusion, hot isostatic pressing or explosive forming. Once structural components are thus formed, the assembly must be performed using techniques that will preserve the desired properties. To do so, the assembly techniques must take on the characteristics of RSP. The CDW process represents a commercial RSP joining technology that is easily studied and reproduced in the laboratory (Ref. 1). Through its essentially one-dimensional action (thermal gradient and heat flow) and very high solidification speed, welds attain quenching rates far in excess of 10^3 K/s.

Solidification processing is well known and many studies are documented in standard texts (Refs. 2, 3), as well as the international technical literature. While RSP is an extension of classical solidification processing, it has become a very active field of research. In the application of welding technology to rapidly solidified materials, consideration must be given not only to the molten or weld zone, but also to the heat-affected zone (HAZ). Review articles by H. Jones (Ref. 4) and Liebermann, *et al.* (Ref. 5), not only described several RSP techniques and their capabilities, but also summarized several attempts at modeling these processes. In 1982, Boettinger (Ref. 6) delineated the importance of growth kinetics in the development of the microstructure of RSP alloys. He also linked the theory of RSP of materials to the older theory of classical solidification processing and defined its boundaries.

Weldability of consolidated RSP powders was studied in 1988 by Clark and Korth (Ref. 7). They compared several welding processes, including CD welding, with gas tungsten arc (GTA) welding of consolidated vacuum gas atomized (VGA) and centrifugally atomized (CA) Type 304 stainless steel powders. They found that CDW and other fusion welding techniques developed microporosity in CA powders due to dissolved He. They also modeled the thermal history of the fusion welded samples using finite element computer codes developed by Kraus (Ref. 8). With this modeling they concluded that CDW and electron beam welding (EBW) produced cooling rates far in excess of those found in the original consolidated powders. They noted a cellular solidification structure of the CD weld and some welds with

KEY WORDS

Capacitor Discharge
CWD
Photographic Analysis
Ultrahigh Speed
RSP Alloys
Transient Phenomena
Expulsion
Plasma Jet
Anode/Cathode Heat
Metal Spatter

R. D. WILSON is a Materials Engineer and J. R. WOODYARD, Sr., is a Physicist, Albany Research Center, U.S. Bureau of Mines, Albany, Ore. J. H. DEVLETIAN is a Professor, Oregon Graduate Institute of Science and Technology, Beaverton, Ore.

Fig. 1 — Capacitor discharge welding process used to join 6.35-mm Fe_3Al solid cylinders with 100 V, 0.08 F, 50-mm drop and 0.9-mm tip length.

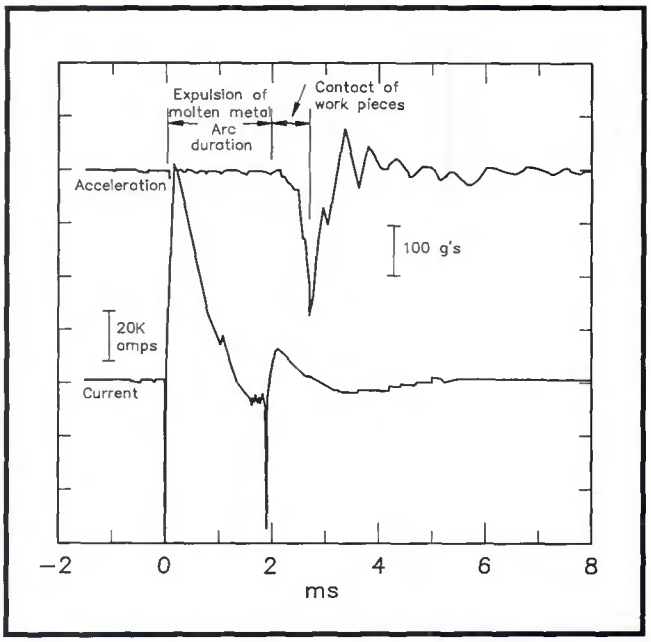

Fig. 2 — Electrical current and acceleration of the capacitor as a function of discharge time. The current increase at 2.5 ms is due to a reduction in circuit resistance on electrode contact

incomplete fusion with visible gaps and tunnels at the weld interface. They used values of the solidification rate, R, the temperature gradient at the solid-liquid interface, G_L, the cooling rate ($G_L \bullet R$), and the solidification parameter G_L/R calculated from the numerical model to determine stability of the interface and predict the solidification mode: planar, cellular, or dendritic. They were able to compare the cooling rates during solidification thus obtained with the primary dendrite arm or cell spacing to confirm the model validity.

In 1987, first Clark, *et al.* (Ref. 9), and then Einerson, *et al.* (Ref. 10), reported detailed studies of CD welding using electrodes prepared from RSP Type 304 stainless steel prepared with CA and VGA. Once again the process was modeled using a one-dimensional, finite element code. They reported the following:

1) Metal spatter from the weld was caused by extrusion as the two electrodes made contact. There was a unequal anode/cathode heating ratio with about twice as much material expelled from the positive electrode as from the negative indicating a ⅔–⅓ heat distribution.

2) Arc spread upon ignition was sufficiently fast that the whole process could be treated as effectively one dimensional.

3) No relationship was found between spatter vs. arc duration, energy, or weld thickness.

4) Calculations from their one-dimensional model agree well with fast cooling rate data (6×10^7 K/s) weld thickness, but not for slow cooling rate data (10^6 K/s), and very poorly for predicted spatter. The model predicts a different spatter in the two high cooling rate cases, but the data do not confirm this.

5) Average temperature gradients are on the order of 10^4 K/mm.

6) Cooling rates predicted by the model show different values for high and low cooling rate cases, but dendritic arm spacing data show no difference in cooling rate for the two cases.

7) Cooling rates are on the order of 10^5 to 10^6 K/s. CD welds can produce fusion zone solidification structures as fine or finer than the original RSP product.

Venkataraman and Devletian (Ref. 11) did a study in 1988 of 304, 316, and 308 stainless steels under CD welding. They optimized the welding parameters to produce both the best fusion and the most rapid quenching rates. They reported the following:

1) Weld thickness decreased with increasing drop height and decreasing ignition tip length (*i.e.*, weld duration).

2) Decreasing voltage on the capacitor also decreased weld thickness, but the optimum voltage for good joining was 90 V.

3) Drop weight did not have a significant effect.

4) Average weld thickness increased proportionally to the square root of the arc time.

5) The total amount of molten metal was much greater than that present in the weld, due to expulsion as spatter.

6) Raising the power density increased the cooling rate during solidification and reduced the dendrite arm spacing of the weld metal.

7) Ignition tip length and drop height were the most effective controllers of weld arc time.

8) The strong dependence of the weld thickness on the arc time despite different heat inputs could be related to the fact that the most superheated liquid was the most likely to be expelled from the weld pool during impact of the contact surfaces.

Metallurgical characterization of the alloys solidified by the CD technique have been adequately described in the literature (Refs. 12, 14), but more information is needed about the CDW process itself. This paper reports a detailed study of the CDW process using ultra-high-speed photography. Although the welding was performed with electrodes made from iron-aluminides, the portion reported here is of general validity and can be expected to hold for other materials as well. The materials and experimental procedures used are first described below. Results of the tests, including the high-speed photography of

CD welds, are described. A summary and conclusions drawn from this work are presented.

Materials and Experimental Procedure

The electrodes used for the CDW experiments were prepared from $Fe_{76}Al_{24}$ intermetallic alloy. Vacuum induction melting was used to cast 150 X 76 X 13-mm (6 X 3 X 0.5-in.) flat plates. Cylindrical electrodes 6.35 mm (0.25 in.) in diameter and 51 mm (2 in.) long were machined from the plates. The electrodes were wrapped in stainless steel foil and homogenized at 1000°C (1832°F) for 1 h, heat treated at 540°C (1004°F) for 100 h, and slowly cooled at 2°C/min (3.6°F/min) to ambient temperature. This heat treatment was used to produce maximum DO_3 long-range order. One electrode from each pair was machined with an electric arc initiation (ignition) tip at the center of the electrode. The ignition tips were 0.635 mm in diameter and cylindrical in shape. The specimens were weighed before and after welding to determine the amount of expelled weld metal for each CD weld.

Since a number of excellent descriptions of the CDW process appear in the literature (Refs. 12–14), only a brief description is given here. Figure 1 depicts the apparatus used in CDW. One anode is fixed in the bottom mount while the cathode is mounted in the gravity drop fixture with a preset weight added. The electrodes are connected to a large, fully charged capacitor bank. For this study, the capacitance was 0.08 F with an open circuit potential of 100 V. The drop weight was 3.88 kg (8.5 lb), and the drop height was 5.08 cm (2 in.). Ignition tip lengths were: P4 — 1.40 mm; P7 — 1.65 mm. For some of the welds, current and time tracings were made (Fig. 2) to help determine the power curve for purposes of modeling the process. In all cases, ultrahigh-speed photographs were made using a high-speed camera operating up to 44,000 frames per second. Both the CDW machine and high-speed camera were operated manually with care to have exposure as close to the maximum frame rate as possible. Table 1 lists the photographic parameters associated with each run. Metallography was performed on each CD weld to assess weld metal thickness and solidification structures. The etchant used for Fe_3Al was a mixed acid etch consisting of 50% acetic acid, 33% HNO_3 and 17% HCl.

Results and Discussion

In assessing the experimental characteristics of the CDW process, full penetration welds were produced using different welding variables. Examination of the fractured surface of the broken weld shown in Fig. 3 illustrates the fusion surfaces similar to those reported in Ref. 5. Figure 3 depicts the fractured surface along the weld centerline of a CD weld in iron aluminide. In this case some of the weld areas solidified prior to electrode contact. The fluid flow patterns illustrate the direction of metal flow as a result of plasma jet impingement on the anode. Figure 4, consisting of a series of frames up to and including elec-

Table 1 — CDW Conditions for the High-Speed Film Experiments Using 100 V, 0.08 F, and a 50-mm Drop Height

CDW Conditions	Exposure — P4	Exposure — P7
Tip length, mm	1.40	1.65
Drop height, m	0.050	0.050
Frame speed, frames/s	44,000	44,000
Voltage	100 V	100 V
Capacitance, F	0.08	0.08
Peak current, I, A	320,000	800,000
μ_o, permitivity of free space	$4\pi \times 10^{-7}$ Kg/C^2	$4\pi \times 10^{-7}$
Arc forces, N	5,120	32,000
Area, w^2	3.16×10^{-5}	3.16×10^{-5}
Arc, pressure	1.62×10^8 N	1.01×10^9, m^2

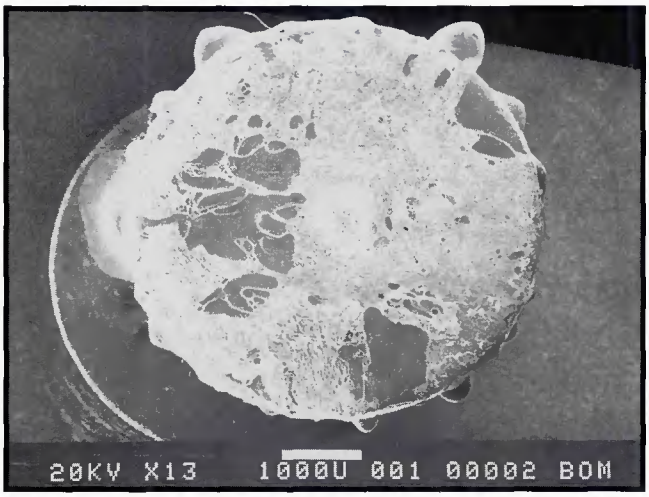

Fig. 3 — Fracture surface of a CD weld after tensile testing.

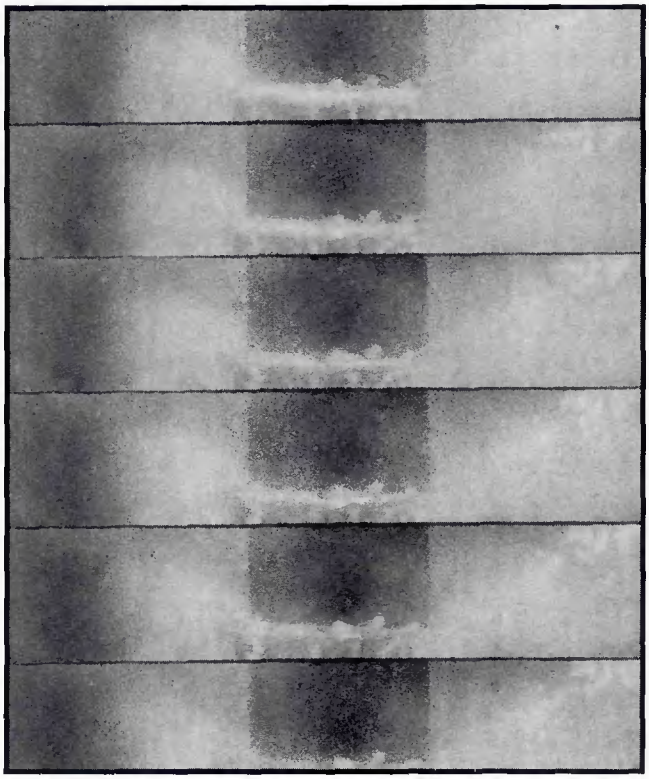

Fig. 4 — High-speed photography of the CDW process. In this series of photographs, the liquid droplet velocity was measured to be 35 m/s. A tip length of 1.65 mm, 100 V, and 0.08 F were used.

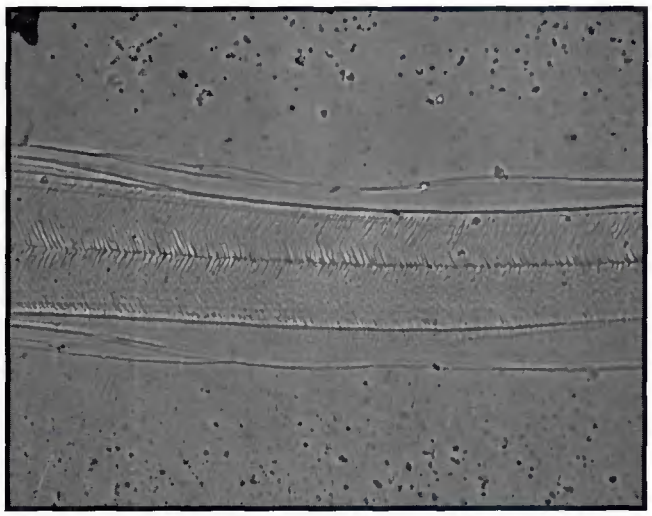

Fig. 5 — CD weld deposited on Fe_3Al. Tip length of 1.4 mm, 100 V, and 0.08 F. The weld thickness is 0.04 mm and the cell spacing is approximately 1.3 μm corresponding to a cooling rate of 5 X 10^5 °C/s. 500X.

trode contact, shows that the molten metal is not "squeezed out on contact" as described in Refs. 9–11, but rather is dynamically expelled from the anode by the plasma jet. The photomicrograph of Fig. 5 shows a cross-section of the CD weld in Fig. 4. It is significant that two planar solidification fronts are formed on either side of the weld centerline. The high-speed movies suggest a difference in heating ratio between the cathode and the anode as reported in Refs. 9 and 10. High heat inputs and long tip lengths result in a formulation of a double planar solidification.

One of the fundamental precepts in the model used in Refs. 8 and 9 was the one dimensionality of the CDW process. From Fig. 6, which consists of several frames showing arc ignition and the spread across the faces of the electrodes, it can be seen that ignition does not take place until contact between electrodes is actually made by the electronic ignition tip. This is confirmed by timing the electrode drop and by calculations of the arc jump length in air at 100 V. The arc spreads across the face of the electrodes in 3 frames or 68 μs, for a total observed welding duration of 94 frames or 1.88 ms. The arc spread represents only 3.6% of the total weld time, indicating the CDW process is essentially one dimensional.

The fine solidification substructure associated with RSP is revealed in the optical micrograph of the weld in Fig. 7. Primary cell spacings are compatible with the 10^5 to 10^6 K/s cooling rates mentioned in Refs. 10 and 11. The spatter mechanism remains the only significant phenomenon affecting solidification structure that needs to be explained more rigorously than has been done in the literature. The mechanism of the melt spatter has been shown to be due, not to extrusion of the metal upon contact of the electrodes, but rather by ejection of melt during the arc in progress. This phenomenon is important because more than 50% of the weld pool may be lost, resulting in increased cooling rates during solidification and reduced dendrite arm or cell spacing.

In gas metal arc welding (GMAW), DC straight polarity produces welds with deep and narrow penetration (Refs. 3, 4). Approximately 70% of the heat is concentrated at the work end and 30% at the electrode end. Burleigh and Eagar (Ref. 15) measured the force exerted by

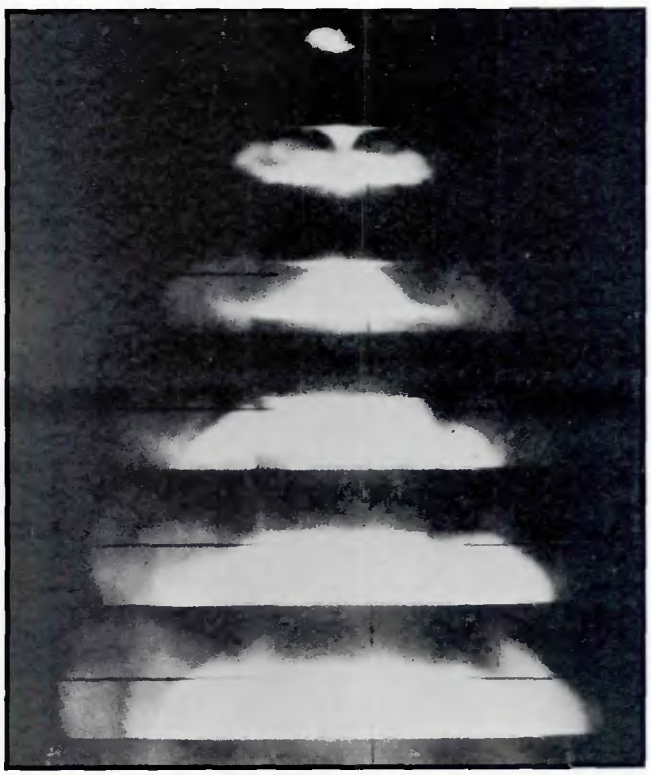

P-4-1 — P-4-5

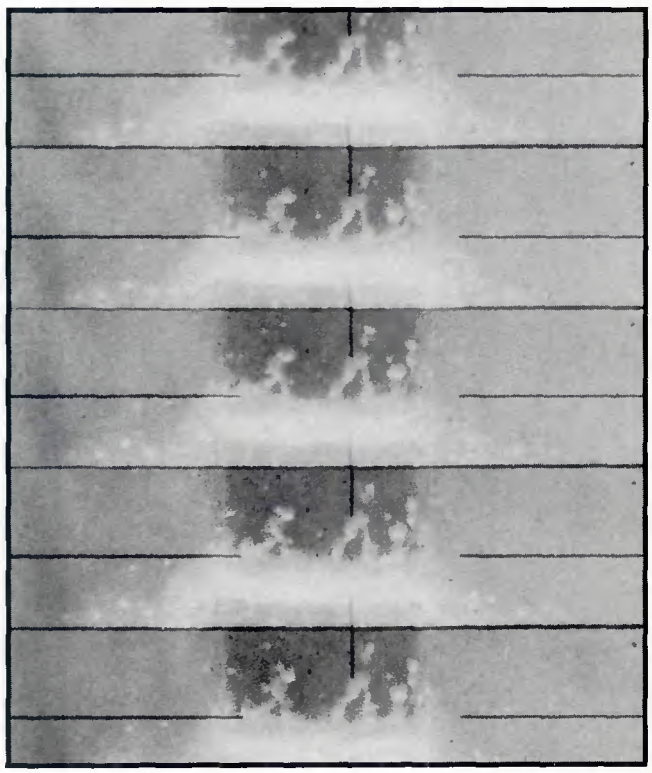

P-4-38 — P-4-42

Fig. 6 — Frames P-4-1 through P-4-5 show the plasma being expelled from a CD weld during the ignition cycle with a 1.4-mm-long ignition tip, 100 V, and 0.08 F. Frames P-4-38 through P-4-42 illustrate the expulsion of metal vapor and liquid material.

a welding arc and found that the measurements were compatible with theory and the arc force is directly proportional to the square of the current (I). For the case of two flat-faced cylindrical electrodes of the same diameter with a linear, one dimensional arc, the proportionality constant is simply (ρ) the permeability of free space divided by 8 π.

$$F_{arc} = \frac{\rho I^2}{8\pi}$$

Calculations show that for the conditions exhibited in the CDW process the pressure exerted by the arc is of the order of 10^9 N/m^2. At such high pressure, all but the most viscous liquids will be expelled from the face of the electrode. Therefore, expulsion of excess melt from the CD welding process will come not primarily from extrusion at the instant of closure, but from continuous ejection by the plasma jet throughout the welding process. This ejection will emanate predominantly from the face of the anode, because the electron current is responsible for the plasma jet. In a time sequence analysis of the CDW process it was found that current flow is initiated upon contact of the ignition tip with the other electrode. The current is sufficient to vaporize the ignition tip and create a dilute plasma. However, the possibility exists that expelled metal is a result of vaporization. In other high-speed photographs, the tip was observed to be buckling and melting while metal vapor and particles were expelled from the anode. The tip remained visible for over 40 frames. The vaporization of the tip seemed to play a minor role in the expulsion of metal during the CDW cycle. The plasma is sufficient to maintain current flow throughout the arcing period.

Electrons and ions fall through the potential drop across the arc (usually on the order of 100 V) and impact on the anode and cathode, respectively. The ions are large, heavy and slow and thus easily stopped by their interaction with the cathode. Their energy is therefore delivered only to the outermost layer of the cathode. The ion current is relatively weak, so material loss from the cathode is primarily from vaporization of the surface layers. The electron current is greater and causes melting of the anode through a much deeper zone than in the case with the cathode. The plasma jet pressure is of the order of 10^9 N/m^2 so any metal reaching the liquidus temperature will be swept away almost instantly. Only surface tension forces act to retain liquid attached to the electrode. This metal leaves the anode at temperatures slightly above the liquidus temperature thereby cooling the anode. Such cooling may be sufficient to reduce the temperature of the face of the electrode to below the liquidus temperature.

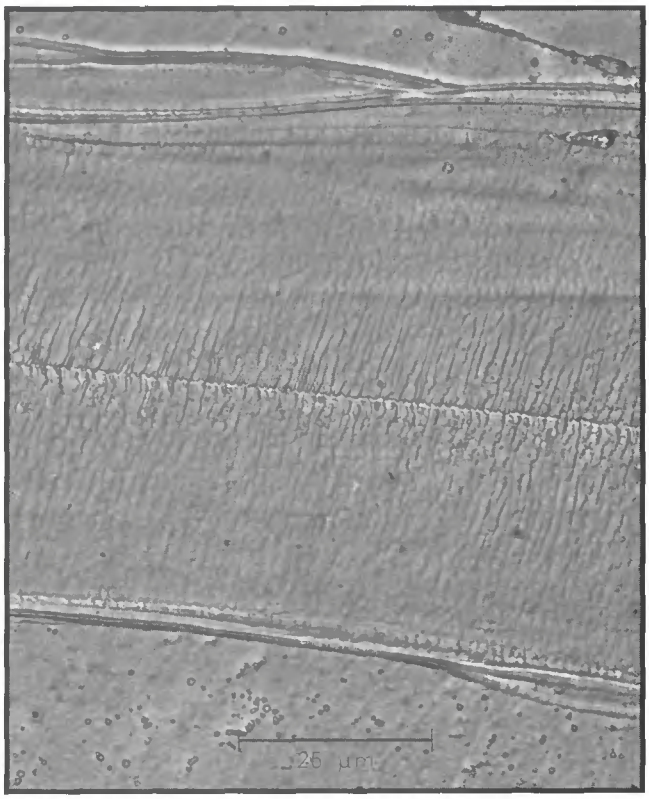

Fig. 7 — Fe_3Al weld deposited by CDW using the short (0.63-mm) ignition tip. The cell spacing is 1.0 μm corresponding to a cooling rate of 5 X 10^5 °C/s. 500X.

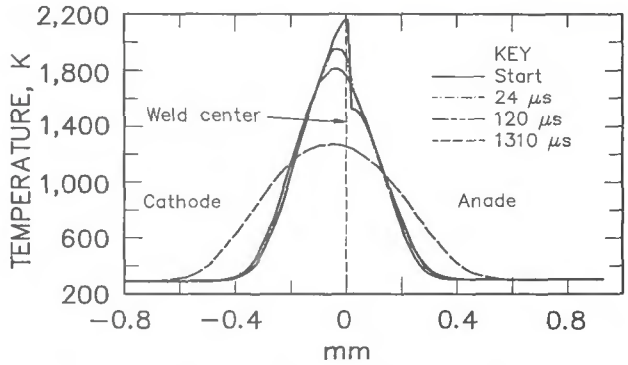

Fig. 8 — Predicted temperature profiles across a CD weld joint at different times during the welding cycle. Heat input was 36 J and the total welding time was 1.31 ms.

A model based on modifications of the computer program SINGLE developed by Kraus (Ref. 7) has been developed to quantify this observed phenomena. Results are in extremely good agreement with current observations, and the results depicted in Figs. 8 and 9 show the solidification predictions for the anode and the cathode.

As the capacitor discharges, the total energy input into the system decreases almost linearly. This has the effect of allowing relative cooling of each electrode as the arcing time reaches the end of the discharge cycle as signified by closure of the electrode gap. Conductive heat transfer will serve to bring each electrode to distribution with the highest temperature at the electrode face — Fig. 8. The anode temperature is significantly lower than the cathode temperature due to the significant loss of heat and material from the anode during the CDW cycle. The rate at which the power input drops is critical to the final temperature distributions.

Upon electrode contact, the cathode

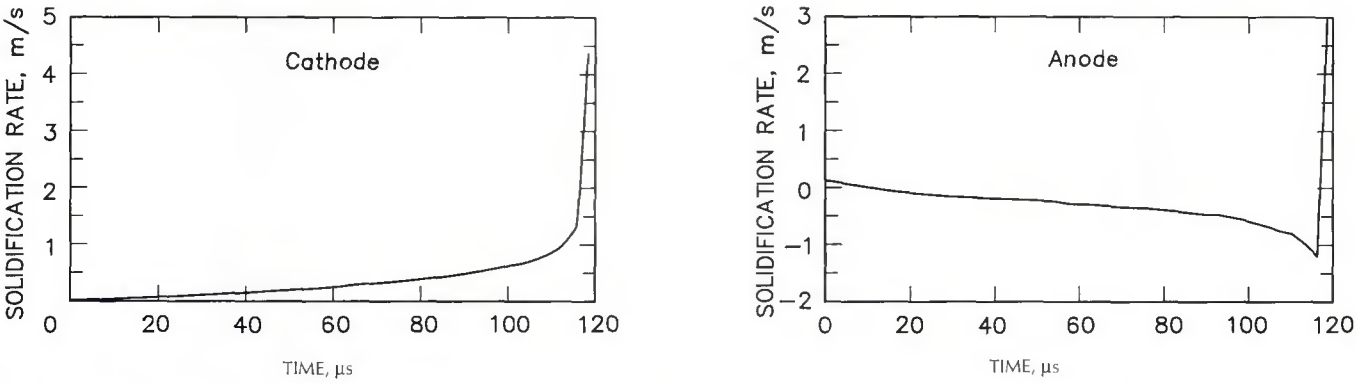

Fig. 9 — Predicted solidification rates for (A) the cathode and (B) the anode as a function of time for CD welds using 36 J heat input to join 6.4-mm-diameter cylinders of Fe_3Al. Total welding time was 1.31 ms.

is at a significantly higher temperature than the anode — Figs. 8, 9. In fact, preliminary calculations indicate that the anode may remain below the liquidus temperature, so the arc will heat the anode somewhat, but really will serve to polish it through the action of the plasma jet. The severe discontinuity in the weld temperature distribution will be reduced very rapidly as thermal conductivity will smooth the distribution. However, the centroid of the distribution will be moved well toward the cathode side. A small amount of melted metal may be expected to be extruded from the cathode upon contact, but close review of the predicted temperature distribution at contact indicates that this will be a very small amount. With the anode at temperature less than the liquidus, poor fusion could be expected, with the expelled metal adhering in the form of small beads at the end of runnels as observed in Fig. 3. Since the temperature gradients are very sharp, the cooling rates and the growth velocity of the solidification front are also very large. As a result weld thickness is small.

Conclusions

An explanation of CD welding has been presented in which the plasma jet from the cathode is seen to dynamically expel melted metal from the anode during the arcing time. This metal expulsion causes cooling of the anode. The following can be concluded about the mechanisms by which CD welding takes place:

1) Metal spatter from the weld is not caused by extrusion upon contact of the electrodes, but rather is caused by expulsion by the plasma jet during the arcing time.

2) The unequal anode/cathode heating ratio is primarily due to the heat transfer from the anode to the metal particles sprayed by the plasma jet.

3) Arc spread upon ignition is fast enough to define the CDW process as essentially one dimensional.

Acknowledgments

The authors wish to acknowledge the contribution of S. T. Anderson, photographer at the Albany Research Center, for his fine work in obtaining the ultra-high-speed photographs of the CD welding process. They also wish to thank H. G. Kraus for providing a copy of the finite element code SINGLE/CE and much instruction on its use, and C. J. Einerson for providing subroutines and modifications for SINGLE/CE used in her research.

References

1. Venkataraman, S., and Devletian, J. H. 1990. Principles of solidification and materials processing. *Proc. Indo-U.S. Workshops*, eds. R. Trivedi, J. A. Sekhar, I. Maazumdar, p. 859, Tech Trans Publications.

2. Flemings, M. C. 1974. *Solidification Processing*. McGraw-Hill.

3. Kurz, W., and Fisher, D. J. 1989. *Fundamentals of Solidification*, p. 305, Vermont, Trans Tech Publications.

4. Jones, H. 1987. Processing of structural metals by rapid solidification. *ASM Conf. Proc.* eds. F. H. Froes and S. J. Savage, P. 77.

5. Liebermann, H., and Walter, J. 1982. *Rapidly Solidified Amorphous and Crystalline Alloys*. ed. B. H. Kear, *et al.*, p. 111, Elsevier Science Pub. Co.

6. Boettinger, W. J. 1982. "Growth" kinetic limitations during rapid solidification. *Rapidly Solidified Amorphous and Crystalline Alloys*. eds. B. H. Kear, B. C. Giessen, and M. Cohen, pp. 15–31, Elsevier Sci. Pub. Co.

7. Clark, D. E., and Korth, G. E. 1988. *Rapidly Solidified Materials: Properties and Processing*. eds. P. W. Lee and J. H. Moll, p. 9.

8. Kraus, H. G. 1983. Interoffice correspondence, p. 1.

9. Clark, D. E., Einerson, C. D., and Loop, R. B. 1987. Internal Report EGC-SCM-7220, INEL, p. 9.

10. Einerson, C. J., Clark, D. E., and Devletian, J. H. 1987. *Proc. of the 1987 ASME/JSME Thermal Engineering Joint Conference* — Volume Three. eds. P. J. Marto, and I. Tanasawa, p. 217. New York, AIME.

11. Venkataraman, S., and Devletian, J. H. 1988. *Welding Journal* 67(6):111-s.

12. Kearns, W. H. 1987. *Welding Handbook*. pp. 261–294, American Welding Society, Miami, Fla.

13. Kou, S. 1987. *Welding Metallurgy*. p. 12. New York, Wiley.

14. Connor, L. P. 1984. *Welding Handbook*. p. 638, American Welding Society, Miami, Fla.

15. Burleigh, T. D., and Eagar, T. W. 1983. *Metallurgical Transactions* 14A: 1223.14.